

Influence of the Modulation Method on the Conduction and Switching Losses of a PWM Converter System

Johann W. Kolar, Hans Ertl, and Franz C. Zach, *Member, IEEE*

Abstract—The optimization of the modulation method of a three-phase pulse-width modulation (PWM) converter system generally does not lead to purely sinusoidal phase modulation functions. In connection with the output currents and the forward characteristics of the electric valves, these phase modulation functions directly define the conduction losses of the power electronic devices. This paper explores the dependency of the conduction losses of a bridge leg of a PWM converter system with a high pulse rate on the shape of the phase modulation functions. This is done for modulation methods that are optimized with respect to minimum harmonic current rms values. The results are compared with the results gained for simple sinusoidal modulation. Besides conduction losses, the switching losses of the electric valves are calculated. Deviations from the classical sinusoidal modulation here are obtained only for modulation methods for which the output voltage is formed by a cyclic change via only two active bridge legs and a third, unswitching bridge leg. As the calculations show, these modulation methods allow a significant increase of the effective switching frequency. This effect is dependent on the phase angle between the fundamental of the converter output phase voltage and the converter output phase current; for this comparison, equal switching losses as for the simple sinusoidal modulation are assumed. The optimal modulation of the pulse frequency of a PWM converter system is treated. A side condition that has to be observed is that the switching power loss has to correspond to the power loss occurring for operation with constant pulse frequency. The optimal modulation as calculated leads to a reduction of the harmonic power loss in the upper modulation region. Furthermore, due to the frequency modulation, the spectrum is spread out to a wider frequency band as compared with the operation with constant pulse frequency; there, the spectrum is concentrated to harmonics in the vicinity of multiples of the pulse frequency. This effect can influence the noise generation of a motor supplied by a converter, for example.

I. INTRODUCTION

IN this section, we want to summarize briefly these modulation methods that will be applied in subsequent calculations. For their characterization the resulting harmonic power losses and the shape of the phase modulation functions are used. Attention is paid especially to the correspondence of the description of the voltage formation using space vector calculus and representation by phase quantities. This is of

Paper IPCSD 91-21, approved by the Industrial Drives Committee of the IEEE Industry Applications Society for presentation at the 1990 Industry Applications Society Annual Meeting, Seattle, WA, October 7-12. Manuscript released for publication February 19, 1991.

The authors are with the Technical University Vienna, Power Electronics Section, Vienna, Austria.

IEEE Log Number 9102112.

special importance here because the determination of conduction and switching losses (which can be linked to a certain modulation method) of a PWM converter system (see Fig. 1) corresponds directly to phase quantities (phase currents or phase modulation functions); furthermore, the optimization of the frequency modulation (which is discussed at the end of the paper) is essentially connected to a description of the system quantities by space vectors. The definition of the converter voltage space vector is given by

$$\underline{u}_U = \frac{2}{3} [u_{U,R} + \underline{a}u_{U,S} + \underline{a}^2u_{U,T}] \quad \underline{a} = \left(-\frac{1}{2} + j\frac{\sqrt{3}}{2} \right). \quad (1)$$

If purely sinusoidal converter output voltage is postulated according to

$$\underline{u}_U^* = \hat{U}_U^* \exp j\varphi_U \quad \varphi_U = \omega_N \tau \quad (2)$$

the control signals for the power semiconductor devices can be derived in the simplest case, as shown in Fig. 2, by "sampling" sinusoidal phase modulation functions

$$\begin{aligned} m'_R(\varphi_U) &= M \cos \varphi_U \\ m'_S(\varphi_U) &= M \cos \left(\varphi_U - \frac{2\pi}{3} \right) \\ m'_T(\varphi_U) &= M \cos \left(\varphi_U + \frac{2\pi}{3} \right) \end{aligned} \quad (3)$$

with

$$M = \frac{2\hat{U}_{U,(1)}^*}{U_{ZK}} = \frac{2\hat{U}_U^*}{U_{ZK}} = M_{(1)} = M_1 \quad M \in [0, 1] \quad (4)$$

(see Fig. 3). The angle φ_U (or time τ) denotes the position of the resulting converter voltage space vector or the position of the corresponding pulse interval within the fundamental period. There, the considerations are limited to the treatment of the voltage fundamental or to the average value for one pulse period or for half a pulse period. One full pulse period is used for symmetric regular sampling and half a pulse period is used for asymmetric regular sampling (Ref. [1]). This distinction is not important here, however, due to the high pulse rate assumed.

This method (known as *subharmonic modulation*) leads to relative turn-on times (related to the pulse period) of the converter bridge legs (which can be replaced by three

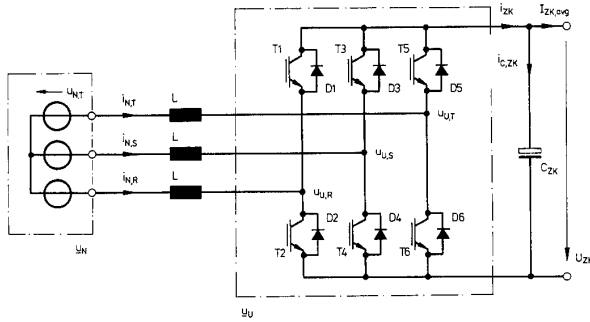


Fig. 1. Structure of the power circuit of a three-phase voltage dc link PWM converter system. For use as PWM inverter for ac machine drives, the inductances L and the three-phase system \underline{u}_N can be interpreted as simple equivalent circuit of the ac machine formed by leakage inductances and machine counter emf. On the other hand, for mains operation of the PWM converter (PWM rectifier, static VAR compensator), the inductances have to be connected in series; the voltage system \underline{u}_N is defined by the mains conditions.

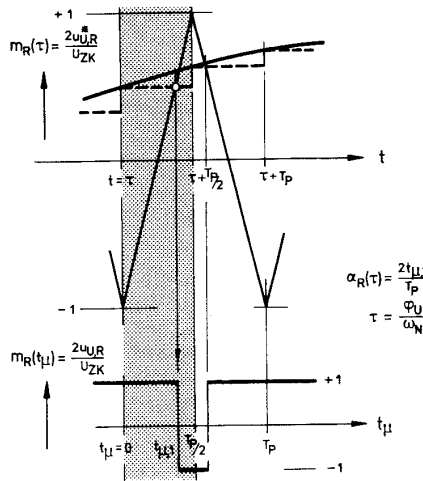


Fig. 2. Derivation of the switching times of a converter bridge leg via intersection of the relevant phase modulation function with a triangular signal (shown for asymmetric regular sampling).

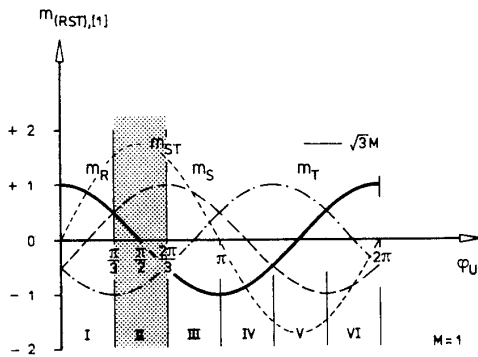


Fig. 3. Shape of the phase modulation functions for the classical sinusoidal modulation (denoted by modulation method [1] in this paper).

double-pole switches between positive and negative dc link voltage bus regarding their electrical function) according to

$$\begin{aligned} \alpha_R(\varphi_U) &= \frac{1}{2} [1 + m_R(\varphi_U)] \\ \alpha_S(\varphi_U) &= \frac{1}{2} [1 + m_S(\varphi_U)] \\ \alpha_T(\varphi_U) &= \frac{1}{2} [1 + m_T(\varphi_U)]. \end{aligned} \quad (5)$$

Due to the symmetries of the generated voltage system resulting from the three-phase properties the further considerations can be limited to the interval of the angle

$$\varphi_U \in \left[\frac{\pi}{3}, \frac{2\pi}{3} \right]. \quad (6)$$

By introducing space vector calculus, the relative turn-on times of the bridge legs given by (5) can be described as a weighting (with respect to time)

$$\begin{aligned} \delta_7 &= \alpha_T \\ \delta_6 &= (\alpha_R - \alpha_T) \\ \delta_2 &= (\alpha_S - \alpha_R) \\ \delta_0 &= (1 - \alpha_S) \end{aligned} \quad (7)$$

of the voltage space vectors $\underline{u}_{U,7}$, $\underline{u}_{U,6}$, $\underline{u}_{U,2}$ and $\underline{u}_{U,0}$, which are associated to the switching state of the PWM converter (Fig. 4). The indices denote the converter switching state by the decimal equivalent of the converter switching status vector interpreted as binary number. Therefore (7) defines the transition of a description by phase quantities to a description by space vector calculus. The modulation method is characterized by the switching state sequence

$$\varphi_U \in \left[\frac{\pi}{3}, \frac{2\pi}{3} \right] \quad \dots 0 \ 2 \ 6 \ 7 \Big|_{t_\mu=0} 7 \ 6 \ 2 \ 0 \Big|_{t_\mu=T_p/2} 0 \ 2 \ 6 \ 7 \dots \quad (8)$$

and this sequence in general is denoted as {7620}. In the transition between two subsequent switching states there is always switching of only one bridge leg.

In the space vector representation of the converter voltage the two non-voltage-forming switching states 0 and 7 cannot be distinguished. Therefore, for definition of the converter output voltage by space vector calculus, only the entire freewheeling state period

$$\delta_0 + \delta_7 = 1 - (\delta_2 + \delta_6) \quad (9)$$

can be given. The voltage formation of the converter system (related to the average value for one pulse period T_p) is not influenced by the *distribution* of the freewheeling states within the pulse interval. The definition of a particular distribution of freewheeling states is really the ultimate basis for the definition of phase modulation functions (see (7)). The degree of freedom given can now be applied for the optimization of the modulation method. The quality functional I to be minimized shall be defined as the squared rms value of the

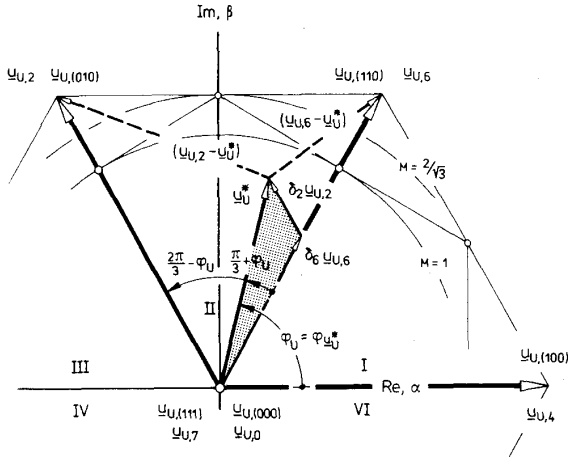


Fig. 4. Approximation of the reference value of the output voltage space vector via neighboring converter voltage space vectors (due to the 60° symmetry of the voltage space vectors following for the different converter switching states one can limit the considerations to the interval of $\varphi_U \in (\pi/3, 2\pi/3)$ shown here).

resulting current harmonics:

$$\begin{aligned}
 I &= \Delta I_{N,rms}^2 \\
 &= \frac{1}{3T_N} \int_{T_N} \left\{ \frac{2}{T_P} \int_{t_\mu=0}^{t_\mu=\frac{T_P}{2}} \right. \\
 &\quad \left. (\Delta i_{N,R}^2 + \Delta i_{N,S}^2 + \Delta i_{N,T}^2) dt_\mu \right\} d\tau \\
 &= \frac{1}{3T_N} \int_{T_N} \Delta i_{N,RST,rms}^2(\tau) d\tau \rightarrow \text{Min.} \quad (10)
 \end{aligned}$$

Equation (10) is obtained with good approximation for PWM converter systems with a high pulse rate (Ref. [2]). For the deviation of the current space vector

$$\Delta i_N = i_N - i_N^* \quad (11)$$

from that of a purely sinusoidal three-phase system

$$i_N^*(\tau) = \hat{i}_N^* \exp j(\omega_N \tau + \varphi) \quad \varphi = \varphi_{u_U^*, i_N^*} \quad (12)$$

we have

$$\frac{d\Delta i_N}{dt_\mu} = \frac{1}{L} [\underline{u}_U^*(\tau) - \underline{u}_U(\tau, t_\mu)] \quad (13)$$

(cf. Ref. [2]) and

$$\Delta i_{N,R}^2 + \Delta i_{N,S}^2 + \Delta i_{N,T}^2 = \frac{3}{2} |\Delta i_N|^2. \quad (14)$$

The minimization of the quality functional I leads to

$$\Delta i_{N,RST,rms}^2(\tau) \rightarrow \text{Min.} \quad (15)$$

There, $\Delta i_{N,RST,rms}^2$ characterizes a ‘‘local’’ (related to a pulse interval) harmonic power loss contribution. It can be set equal to the square of a local harmonic current rms value.

It shows the dependency given by

$$\begin{aligned}
 \Delta i_{N,RST,rms}^2(\tau) &= \Delta i_{N,RST,rms,1}^2 \{ \delta_7(\tau), \delta_6(\tau), \delta_2(\tau) \} \\
 &\quad + \Delta i_{N,RST,rms,2}^2 \{ \delta_6(\tau), \delta_2(\tau) \} \quad (16)
 \end{aligned}$$

on the weighting with respect to time of the different converter voltage space vectors. The optimal phase modulation functions follow (as also discussed in Ref. [3]) as

$$\begin{aligned}
 m_R(\varphi_U) &= M_1 \cos \varphi_U - M_3 \cos 3\varphi_U \\
 m_S(\varphi_U) &= M_1 \cos \left(\varphi_U - \frac{2\pi}{3} \right) - M_3 \cos 3\varphi_U \\
 m_T(\varphi_U) &= M_1 \cos \left(\varphi_U + \frac{2\pi}{3} \right) - M_3 \cos 3\varphi_U \quad (17)
 \end{aligned}$$

with

$$\begin{aligned}
 \frac{M_3}{M_1} \Big|_{I=\text{Min}} &= \frac{1}{4} \\
 M_3 &= \frac{2\hat{U}_{U,(3)}^*}{U_{ZK}} \left(M_{1,\text{Max}} \Big|_{\frac{M_3}{M_1} = \frac{1}{4}} = 0.972 \frac{2}{\sqrt{3}} \right). \quad (18)
 \end{aligned}$$

The corresponding phase modulation functions are shown as modulation method [3] in Fig. 5. For the global (as related to the fundamental period) harmonic current rms value we have, in general, with (15), (16), and (10):

$$\begin{aligned}
 \Delta I_{N,rms,[3]}^2 &= \frac{1}{6} \Delta i_n^2 M_1^2 \left\{ 1 - \frac{8M_1}{\sqrt{3}\pi} \right. \\
 &\quad \left. + \frac{3M_1^2}{4} \left[1 - \frac{M_3}{M_1} \left(1 - 2\frac{M_3}{M_1} \right) \right] \right\} \quad (19)
 \end{aligned}$$

with

$$\Delta i_n = \frac{U_{ZK} T_P}{8L} \quad (20)$$

(cf. modulation method [3] in Fig. 6). The maximum modulation region

$$M \in \left[0, \frac{2}{\sqrt{3}} \right] \quad (21)$$

follows for $M_3/M_1 = \frac{1}{6}$ (see Refs. [2] and [4]).

A simple suboptimal approximation (denoted by modulation method [2] in this paper) can be given by distributing the freewheeling state to equal parts at the beginning and at the end of each pulse half-interval according to

$$\delta_{7,[2]} = \frac{1}{2} (\delta_0 + \delta_7) = \frac{1}{2} [1 - (\delta_2 + \delta_6)] \quad (22)$$

(see Refs. [2] and [5]). For the global harmonic rms value there follows

$$\begin{aligned}
 \Delta I_{N,rms,[2]}^2 &= \frac{1}{6} \Delta i_n^2 M^2 \left[1 - \frac{8M}{\sqrt{3}\pi} + \frac{9M^2}{8} \left(1 - \frac{3\sqrt{3}}{4\pi} \right) \right] \\
 &\quad \cdot M \in \left[0, \frac{2}{\sqrt{3}} \right]. \quad (23)
 \end{aligned}$$

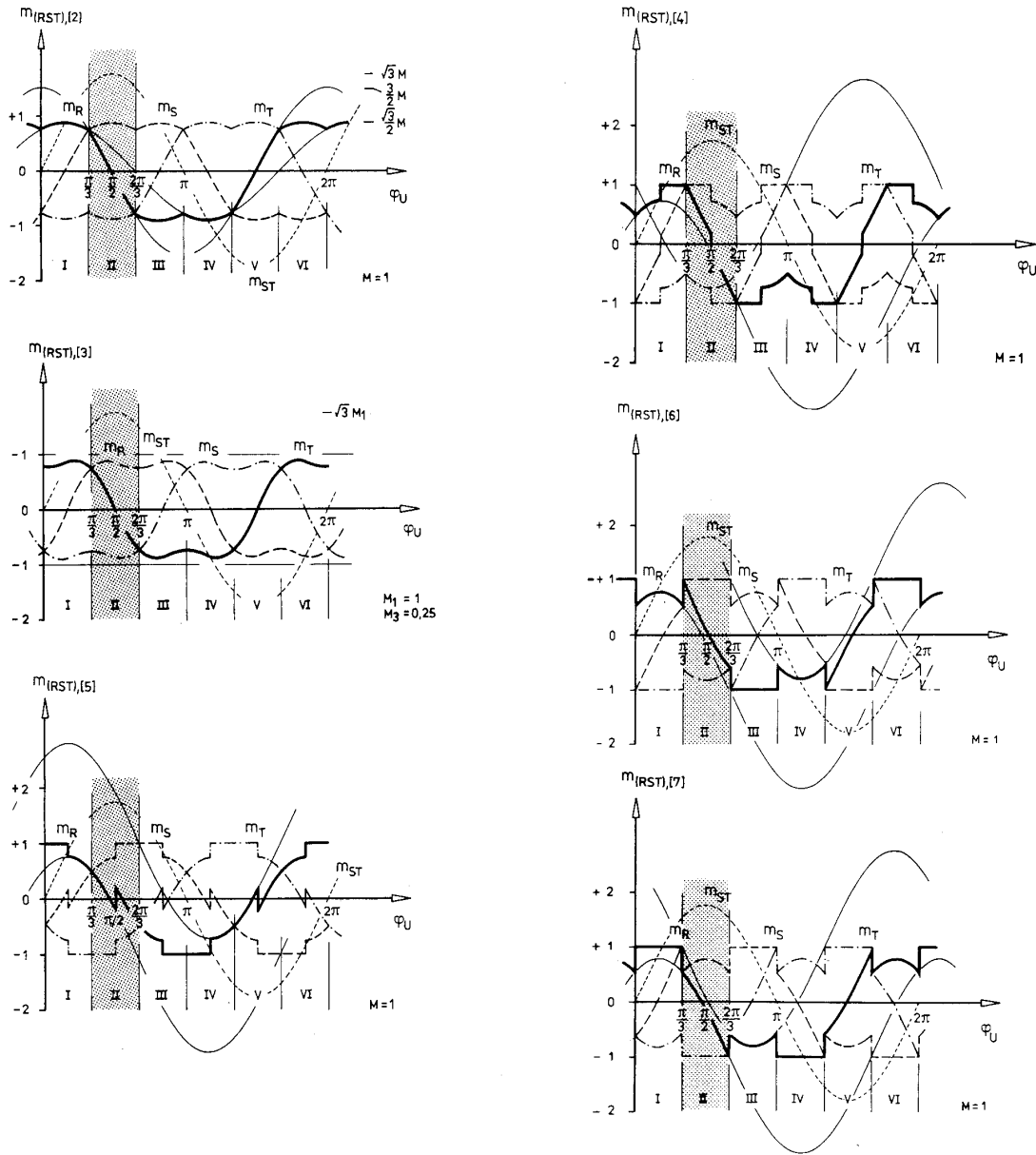


Fig. 5. Illustration of the modulation methods discussed in this paper via representation by the corresponding phase modulation functions: [2] and [3]: continuous modulation; [4]-[7]: discontinuous modulation).

As already mentioned, for a simple sinusoidal modulation (denoted by modulation method [1]) the distribution of the freewheeling states is determined directly by the shape of the phase modulation functions. It follows as

$$\delta_{7,[1]} = \frac{1}{2} + \frac{M}{2} \cos\left(\varphi_U + \frac{2\pi}{3}\right). \quad (24)$$

In this case we have, for the global harmonic rms value,

$$\Delta I_{N,rms,[1]}^2 = \frac{1}{6} \Delta i_n^2 M^2 \left[1 - \frac{8M}{\sqrt{3}\pi} + \frac{3M^2}{4} \right] \quad \text{or} \quad M \in [0,1]. \quad (25)$$

As a limiting case of the distribution of the freewheeling states as discussed, we also have a formation of the switching state sequence according to

$$\begin{aligned} \delta_7 &= 1 - (\delta_2 + \delta_6) \\ \delta_0 &= 0 \end{aligned} \quad (26)$$

$$\dots 2 \ 6 \ 7 \mid_{t_{\mu=0}} 7 \ 6 \ 2 \mid_{t_{\mu=T_p/2}} 2 \ 6 \ 7 \dots \{762\} \text{ or } [6] \quad (27)$$

$$\begin{aligned} \delta_7 &= 0 \\ \delta_0 &= 1 - (\delta_2 + \delta_6) \end{aligned} \quad (28)$$

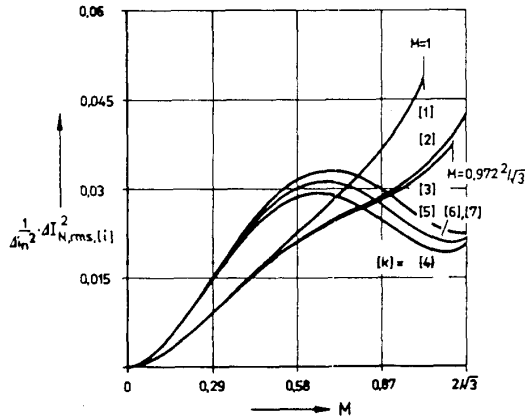


Fig. 6. Comparison of the normalized harmonic power losses of one phase for various modulation methods (discussed in Section I). [1]: Sinusoidal modulation (25). [2]: Suboptimal space vector modulation (23). [3]: Local and global optimal sinusoidal modulation with added third harmonic ($M_f = M_1/4$, (19)). [4]–[7]: Discontinuous modulation (cf. (30), (32), (34)); $k_{f[4]-[7]} = \frac{3}{2}$.

$$\dots 0 \ 2 \ 6 \mid_{t_\mu=0} 6 \ 2 \ 0 \mid_{t_\mu=T_p/2} 0 \ 2 \ 6 \dots \{620\} \text{ or } [7] \quad (29)$$

that can be considered. There the entire freewheeling state is concentrated at the beginning or at the end of a pulse half-interval. Due to the given nonoptimal “distribution,” there result higher harmonic losses of the system, however. The analysis of the associated phase modulation functions (cf. modulations [6] and [7] in Fig. 5) shows, however, that then, the output voltage system is formed by pulsing of only two bridge legs, whereas the third phase remains “clamped” to one of the two dc link voltage bus bars (*discontinuous modulation*). Accordingly, the conclusion is obvious that an increase of the pulse frequency by a factor $k_f = \frac{3}{2}$ leads to equal switching losses and equal thermal stress on the power semiconductor devices as compared to the case of *continuous modulation* (modulation function without discontinuities, or, equivalent, pulsing of all bridge legs within each pulse (half) interval as used for modulation methods [1]–[3]). A closer investigation shows, however, that the possible frequency increase is determined essentially by the phase relationship between the output current fundamental and the output voltage fundamental. This aspect is treated in Section III in detail. The harmonic losses resulting for the modulation methods given by (26) and (28) (or (27) and (29), respectively) follow as

$$\Delta I_{N,rms,[6],[7]}^2 = \frac{1}{6} \Delta i_n^2 M^2 \frac{1}{k_{f,[6],[7]}^2} \cdot \left[4 - \frac{35M}{\sqrt{3}\pi} + \frac{9M^2}{8} \left(2 + \frac{3\sqrt{3}}{4\pi} \right) \right] \quad M \in \left[0, \frac{2}{\sqrt{3}} \right]. \quad (30)$$

They are shown in Fig. 6 (cf. modulation methods [6] and [7]) for $k_{f,[6],[7]} = \frac{3}{2}$. The possible frequency increase $k_{f,[1]}$

$= f_{P,[1]}/f_P$ therefore leads to a significant harmonic power loss reduction in the upper modulation region, also if compared to optimal continuous modulation.

For a combination (denoted by modulation [4]) of the switching state sequences (given by (27) and (29)) according to

$$\begin{cases} \{762\} & \text{for } \varphi_U \in \left[\frac{\pi}{3}, \frac{\pi}{2} \right] \\ \{620\} & \text{for } \varphi_U \in \left[\frac{\pi}{2}, \frac{2\pi}{3} \right] \end{cases} \quad (31)$$

there follows

$$\Delta I_{N,rms,[4]}^2 = \frac{1}{6} \Delta i_n^2 M^2 \frac{1}{k_{f,[4]}^2} \left[4 - \frac{M}{\sqrt{3}\pi} (62 - 15\sqrt{3}) + \frac{9M^2}{8} \left(2 + \frac{\sqrt{3}}{\pi} \right) \right] \quad M \in \left[0, \frac{2}{\sqrt{3}} \right] \quad (32)$$

(cf. modulation method [4] in Figs. 5 and 6).

An alternative combination (denoted by modulation method [5])

$$\begin{cases} \{620\} & \text{for } \varphi_U \in \left[\frac{\pi}{3}, \frac{\pi}{2} \right] \\ \{762\} & \text{for } \varphi_U \in \left[\frac{\pi}{2}, \frac{2\pi}{3} \right] \end{cases} \quad (33)$$

leads to

$$\Delta I_{N,rms,[5]}^2 = \frac{1}{6} \Delta i_n^2 M^2 \frac{1}{k_{f,[5]}^2} \left[4 - \frac{M}{\sqrt{3}\pi} (8 + 15\sqrt{3}) + \frac{9M^2}{8} \left(2 + \frac{\sqrt{3}}{2\pi} \right) \right] \quad M \in \left[0, \frac{2}{\sqrt{3}} \right] \quad (34)$$

(cf. modulation method [5] in Figs. 5 and 6). Equation (31) defines the harmonic-optimal discontinuous modulation method (cf. modulation methods [4]–[7] in Fig. 6, see also Ref. [2]) based on a possible frequency increase $k_f = \frac{3}{2}$.

Finally, we want to point out that all the modulation functions discussed here can be derived by extension m_0 of a simple sinusoidal modulation $m'_{(RST)}$ according to

$$\begin{aligned} m_R &= m'_R + m_0 \\ m_S &= m'_S + m_0 \\ m_T &= m'_T + m_0 \\ m_0 &= \frac{1}{3} (m_R + m_S + m_T). \end{aligned} \quad (35)$$

Zero quantity m_0 is not projected into the corresponding space vector when the voltage system is transformed (the zero voltage is decoupled); m_0 only influences the distribution of the freewheeling states and therefore the resulting harmonic losses.

II. CALCULATION OF THE CONDUCTION LOSSES OF THE POWER SEMICONDUCTOR DEVICES

The relative conduction periods of the power electronic devices of the bridge legs within a pulse half period are

defined (as mentioned in the introduction) according to

$$\begin{aligned} \alpha_{D1}(\varphi_U) &= \alpha_R(\varphi_U) \\ \alpha_{T2}(\varphi_U) &= 1 + \alpha_R(\varphi_U) \end{aligned} \quad \text{with } \varphi_U = \omega_N \tau \quad (36)$$

(given for phase *R* and limited to the positive current half period; cf. Fig. 7) directly by the shape of the phase modulation functions. If one approximates the forward characteristics of the valves by

$$u_{F,Ti,Di} = U_{F,T,D} + r_{F,T,D} i_{Ti,Di} \quad (37)$$

there follows for the mean value of the conduction losses within one pulse half period ("local" conduction losses, i.e., "local" with respect to time)

$$\begin{aligned} P_{F,D1}(\tau) &= U_{F,D} i_{D1,avg}(\tau) + r_{F,D} i_{D1,rms}^2(\tau) \\ &= U_{F,D} \alpha_R(\tau) i_{D1}(\tau) + r_{F,D} \alpha_R(\tau) i_{D1}^2(\tau) \end{aligned} \quad (38)$$

with

$$i_{D1}(\tau) = i_{N,R}(\tau) = \hat{I}_N \cos(\omega_N \tau + \varphi). \quad (39)$$

The integration of these local conduction losses for the positive half cycle of the output current

$$\begin{aligned} P_{F,D1} &= U_{F,D} \left\{ \frac{1}{T_N} \int_{-\pi/2-\varphi}^{\pi/2-\varphi} \frac{\omega_N}{\omega_N} \alpha_R(\tau) i_{D1}(\tau) d\tau \right\} \\ &\quad + r_{F,D} \left\{ \frac{1}{T_N} \int_{-\pi/2-\varphi}^{\pi/2-\varphi} \frac{\omega_N}{\omega_N} \alpha_R(\tau) i_{D1}^2(\tau) d\tau \right\} \end{aligned} \quad (40)$$

finally leads to

$$\begin{aligned} P_{F,D1} &= \frac{U_{F,D} \hat{I}_N}{2} \left(\frac{1}{\pi} + \frac{M}{4} \cos \varphi \right) \\ &\quad + r_{F,D} \hat{I}_N^2 \left(\frac{1}{8} + \frac{M}{3\pi} \cos \varphi \right) \end{aligned} \quad (41)$$

for the global (i.e., related to the fundamental period) conduction loss. There, simple sinusoidal modulation

$$\alpha_R(\tau) = \frac{1}{2} [1 + M \cos \omega_N \tau] \quad (42)$$

is assumed. Integration for the output current half cycle, therefore, means integration of a quantity $\alpha_{D1}(\tau)$ (or $\alpha_{T2}(\tau)$), which is weighted by the instantaneous current value (and dependent on the position φ_U of the converter voltage space vector) within an interval that is dependent on the phase angle between the fundamentals of the converter output phase voltage and current. For the conduction losses of the transistor T2, which conducts current for positive output current, there follows then (cf. also Refs. [6, 7, 8])

$$\begin{aligned} P_{F,T2} &= \frac{U_{F,T} \hat{I}_N}{2} \left(\frac{1}{\pi} - \frac{M}{4} \cos \varphi \right) \\ &\quad + r_{F,T} \hat{I}_N^2 \left(\frac{1}{8} - \frac{M}{3\pi} \cos \varphi \right). \end{aligned} \quad (43)$$

The purely sinusoidal output current shape being assumed by (39) limits the validity of (41) or (43), together with (38)

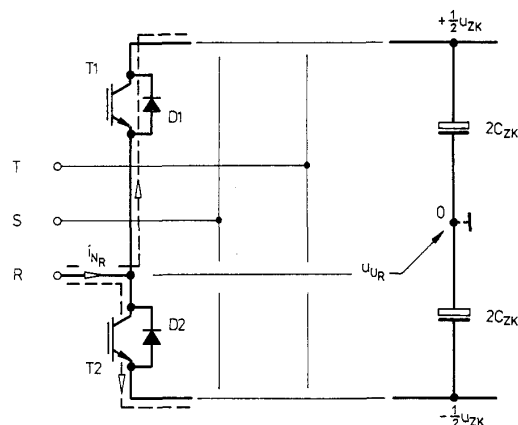


Fig. 7. Division of the output current flowing into controlled and uncontrolled semiconductor devices of a PWM converter bridge leg.

to a region of high pulse numbers pz (ratio of the pulse frequency to the output frequency). It can be used, however, (as a comparison with the results of a digital simulation shows) in practice already for $pz > 21$ with sufficient accuracy for the thermal dimensioning of the valves. In general, dimensioning on the basis of *global* power losses (i.e., averaged over the fundamental period) assumes sufficient (i.e., sufficient for the time of averaging applied, i.e., for the fundamental period) thermal inertia of the power semiconductors. This assumption is sufficiently well fulfilled for PWM rectifier systems for high power (the averaging time is given by the mains fundamental period). For converters used in drives the validity of the relationships derived in this paper is limited to the higher output frequency or modulation region. (There, frequency-proportional change of the output voltage amplitude is usually given.) For low output frequencies, *local* power losses and the transient thermal resistance must be considered for dimensioning.

If the simple sinusoidal modulation is extended by addition of a third harmonic (Refs. [2]–[4]) (see modulation method [3] in Fig. 5 ((17) in Section I)) the relative conduction intervals of the valves are influenced (cf. (36)). For example, there follows, for diode D1,

$$\alpha_{D1}(\varphi_U) = \frac{1}{2} + \frac{M_1}{2} \cos \varphi_U - \frac{M_3}{2} \cos 3\varphi_U. \quad (44)$$

This means that, in any case, a corresponding change of the conduction losses can be expected. The evaluation of (40) under consideration of (39) and (44) leads to

$$\begin{aligned} P_{F,D1} &= \frac{U_{F,D} \hat{I}_N}{2} \left(\frac{1}{\pi} + \frac{M_1}{4} \cos \varphi \right) \\ &\quad + r_{F,D} \hat{I}_N^2 \left(\frac{1}{8} + \frac{M_1}{3\pi} \cos \varphi - \frac{M_3}{15\pi} \cos 3\varphi \right) \end{aligned} \quad (45)$$

and

$$\begin{aligned} P_{F,T2} &= \frac{U_{F,T} \hat{I}_N}{2} \left(\frac{1}{\pi} - \frac{M_1}{4} \cos \varphi \right) \\ &\quad + r_{F,T} \hat{I}_N^2 \left(\frac{1}{8} - \frac{M_1}{3\pi} \cos \varphi + \frac{M_3}{15\pi} \cos 3\varphi \right) \end{aligned} \quad (46)$$

($M_3 = 0.25 M_1$ for optimized PWM (cf. Section I)). The part of the loss that is dependent on the constant conduction voltage representation therefore is *not* influenced by the modulation method modification (cf. (41) and (43)); the part linked to the conduction resistance is influenced only marginally. As can be considered, e.g., graphically in a simple way (cf. Fig. 8), we can write

$$n \int_{\pi} \cos[(2k+1)\varphi_U] \cos[\varphi_U + \varphi] d\varphi_U = 0 \quad k = 1, 2, \dots \quad (47)$$

Therefore, in general for a change of the simple sinusoidal modulation method of odd-order harmonics, or, especially, by a zero quantity m_0 defined by (35) (see modulation methods [2]–[7] in Fig. 5) the conduction losses linked to the not current dependent part of the conduction voltage are not influenced. This means that the calculation can be restricted to the second loss part; as a close investigation of the modulation methods described in Section I shows, this power loss contribution can always be approximated with an accuracy that is sufficient for dimensioning purposes via the expression resulting for sinusoidal modulation. The thermal dimensioning of the power electronic devices regarding global conduction losses, therefore, is only marginally influenced by the shape of the modulation function.

III. CALCULATION OF THE SWITCHING LOSSES

For the calculation of the switching losses related to the modulation methods considered, one assumes (according to the measurement results of Refs. [8]–[11]) a linear dependency of the switching energy loss (appearing for one switching cycle of a bridge leg) on the switched current

$$w_{P,T}\{i_T(\omega_N\tau)\} = k_{1,T}i_T(\omega_N\tau). \quad (48)$$

For the definition of a local switching loss (related to a position of a pulse interval) one can write

$$P_{P,T} = w_{P,T}f_P \quad (49)$$

when a high pulse number is implied.

Averaging

$$P_{P,T2} = \frac{1}{2\pi} \int_{-\pi/2-\varphi}^{+\pi/2-\varphi} P_{P,T2}(\varphi_U) d\varphi_U \quad (50)$$

of this switching loss appearing within the positive (or negative) output current half period leads for *continuous* modulation (e.g., sinusoidal modulation [1], [2], or [3] in Fig. 5) to a global switching loss of a transistor–diode pair of a bridge leg (e.g., T2 and D1 in Fig. 7)

$$P_{P,T2,D1} = \hat{I}_N f_P \frac{k_{1,T,D}}{\pi} \quad (51)$$

with

$$k_{1,T,D} = k_{1,T} + k_{1,D}. \quad (52)$$

The shape of the modulation function basically influences the switching losses only if the various bridge legs are not pulsed within the entire fundamental period with pulse fre-

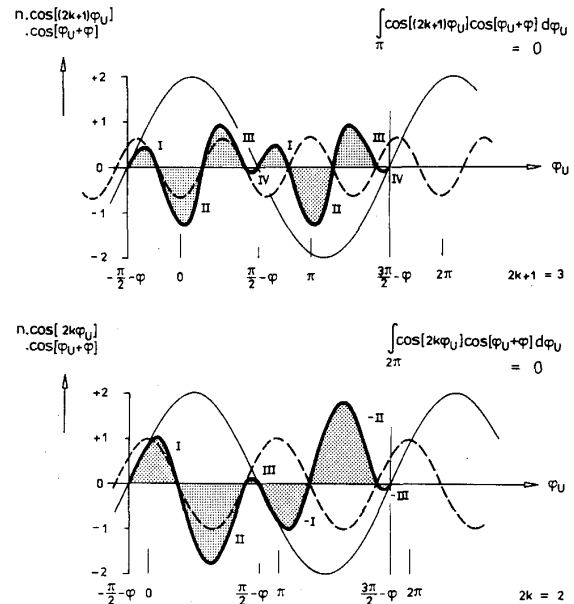


Fig. 8. For derivation of (47).

quency (*discontinuous* modulation, modulation methods [4]–[7] in Fig. 5). As Figs. 9 and 10 show, there has to be decided among different cases in dependency on the phase relationship between the fundamentals of the output phase voltage and current. For the switching losses there follows

$$\begin{aligned} P_{P,T2,D1,[4]} &= \frac{\hat{I}_N k_{1,T,D} f_{P,[4]}}{\pi} \left[1 - \frac{(\sqrt{3}-1)}{2} \cos \varphi \right] \\ \varphi &\in \left[0, \frac{\pi}{6} \right] \\ &= \frac{\hat{I}_N k_{1,T,D} f_{P,[4]}}{\pi} \left[\frac{\sin \varphi + \cos \varphi}{2} \right] \\ \varphi &\in \left[\frac{\pi}{6}, \frac{\pi}{3} \right] \\ &= \frac{\hat{I}_N k_{1,T,D} f_{P,[4]}}{\pi} \left[1 - \frac{(\sqrt{3}-1)}{2} \sin \varphi \right] \\ \varphi &\in \left[\frac{\pi}{3}, \frac{\pi}{2} \right] \end{aligned} \quad (53)$$

$$\begin{aligned} P_{P,T2,D1,[5]} &= \frac{\hat{I}_N k_{1,T,D} f_{P,[5]}}{\pi} \left(1 - \frac{1}{2} \cos \varphi \right) \\ \varphi &\in \left[0, \frac{\pi}{3} \right] \\ &= \frac{\hat{I}_N k_{1,T,D} f_{P,[5]}}{\pi} \frac{\sqrt{3} \sin \varphi}{2} \\ \varphi &\in \left[\frac{\pi}{3}, \frac{\pi}{2} \right] \end{aligned} \quad (54)$$

(values for the other phase angle regions follow via symmetry considerations (cf. Figs. 9, 10, and 11)). Depending on the phase angle of the output current and on the modulation

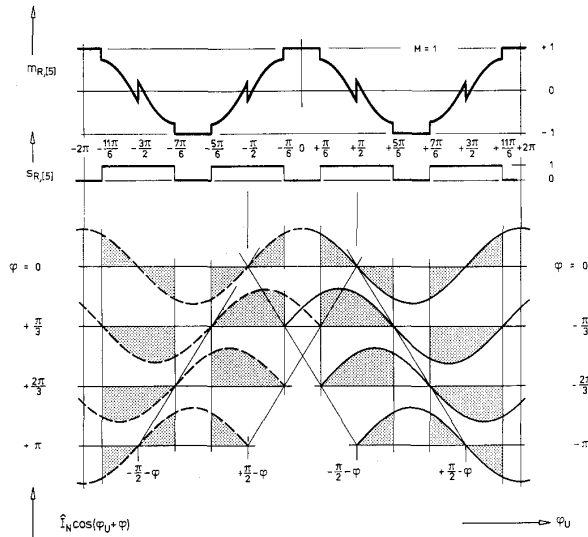


Fig. 9. For derivation of the switching loss dependency on the phase shift between output voltage and output current for modulation method [5]. ($m_{R,[5]}$: phase modulation function (given for phase R); $s_{R,[5]}$: switching frequency status of the bridge leg ($s_{R,[5]} = 1$ for switching bridge leg, $s_{R,[5]} = 0$ for intervals when bridge leg is clamped); lower curves: distinction of different cases for the phase angle regions of the output current).

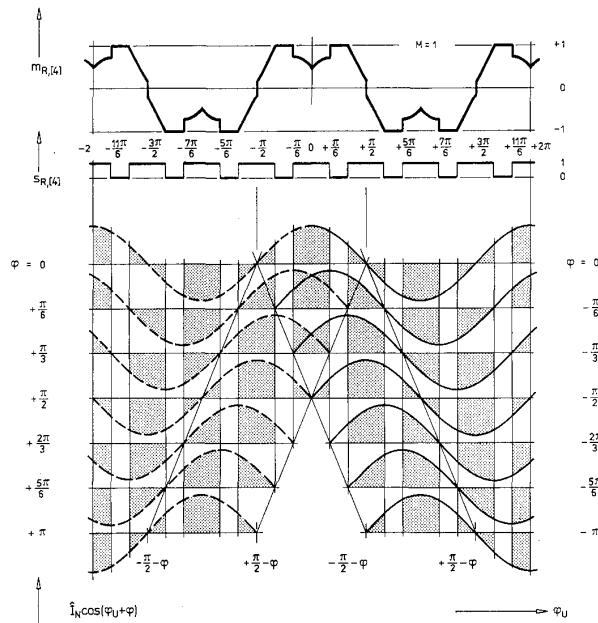


Fig. 10. For derivation of the switching loss dependency on the phase shift between output voltage and output current for modulation method [4]. ($m_{R,[4]}$: Phase modulation function (given for phase R); ($s_{R,[4]}$: switching frequency status of the bridge leg ($s_{R,[4]} = 1$ for switching bridge leg, $s_{R,[4]} = 0$ for intervals when bridge leg is clamped); lower curves: distinction of different cases for the phase angle regions of the output current).

method used ([4] or [5]), this makes possible (cf. Fig. 11) an increase of the "local"¹ pulse frequency ($f_{P,[4]}$ or $f_{P,[5]}$,

¹(The local pulse frequency $f_{P,[i]}$ in this section is given by either $f_P = 0$ for the clamping intervals or by $f_P = f_{P,[i]}$ is constant for the other time intervals of the fundamental period. For additional methods concerning the modulation of the pulse frequency, see Section VI.)

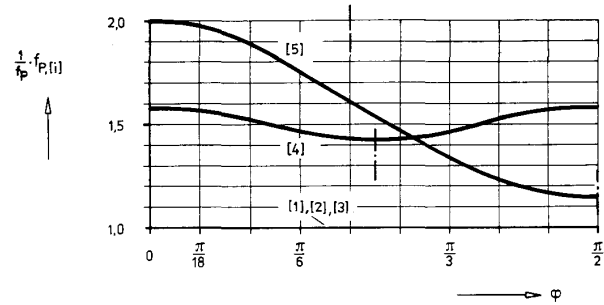


Fig. 11. Possible frequency increase $k_{f,[i]}$ of modulation methods [4] and [5] in comparison to *continuous* modulation methods (e.g., simple sinusoidal modulation [1]) for equal switching losses (as a side condition for comparison purposes).

respectively by a factor of

$$k_{f,[4]} = \frac{f_{P,[4]}}{f_P} = \frac{1}{\left[1 - \frac{(\sqrt{3}-1)}{2} \cos \varphi\right]} \quad \varphi \in \left[0, \frac{\pi}{6}\right]$$

$$= \frac{2}{[\sin \varphi + \cos \varphi]} \quad \varphi \in \left[\frac{\pi}{6}, \frac{\pi}{3}\right]$$

$$= \frac{1}{\left[1 - \frac{(\sqrt{3}-1)}{2} \sin \varphi\right]} \quad \varphi \in \left[\frac{\pi}{3}, \frac{\pi}{2}\right]$$
(55)

$$k_{f,[5]} = \frac{f_{P,[5]}}{f_P} = \frac{1}{\left(1 - \frac{1}{2} \cos \varphi\right)} \quad \varphi \in \left[0, \frac{\pi}{3}\right]$$

$$= \frac{2}{\sqrt{3} \sin \varphi} \quad \varphi \in \left[\frac{\pi}{3}, \frac{\pi}{2}\right]$$
(56)

There, equal global switching loss is assumed as for the case of the simple sinusoidal modulation for which we have equality of "local" and "global" pulse frequency f_P . The shift between the periods where no pulsing of a bridge leg takes place and the associated current fundamental has essential influence on the possible frequency increase. This is true because the calculation of the switching losses (cf. (49) and (50)) is performed by weighting the instantaneous output current value by the local pulse frequency. If a converter phase is clamped to a bus bar voltage within ($\pi/3$)-wide intervals (e.g., cf. (33), or modulation method [5] in Fig. 5), then k_f shows a significant dependency on the phase shift of the output current. If the clamping interval of a phase (i.e., there appear no local switching losses) lies symmetrical to the current maximum ($\varphi = 0$), as is the case for modulation method 5, the local switching frequency can be increased by a factor of 2 as compared to continuous modulation. The frequency increase of $k_f = 1.5$, which could be concluded from a superficial consideration of the problem (independent of the current phase angle, see Section I), therefore, does not represent the maximum achievable value. However, there appear phase-angle regions where the clamping states will be

located in the neighborhood of the current zero crossings ($\varphi = \pi/2$). Then the switching of the bridge legs occurs at high current levels (near or at the current maximum). The possible frequency increase in this case will be given by $k_f \leq 1.5$. If the clamping states are distributed more evenly over the fundamental period, there results—as is immediately clear from previous considerations—a less-pronounced dependency of the frequency increase on the current phase shift (cf. modulation method [4] in Figs. 5 or 11, respectively).

A closer discussion of the discontinuous modulation methods [6] and [7] (cf. Fig. 5), defined in Section I by (26) and (28), can be omitted here because the frequency increase, which becomes possible when these methods are applied, can be derived directly from the relationships calculated for modulation method [5]. This becomes immediately clear by comparing modulation methods [5], [6], and [7] in Fig. 5. We have

$$k_{f,[6]}(\varphi) = k_{f,[5]} \left(\varphi - \frac{\pi}{6} \right) \quad (57)$$

or

$$k_{f,[7]}(\varphi) = k_{f,[5]} \left(\varphi + \frac{\pi}{6} \right). \quad (58)$$

According to the application area of the PWM converter system (phase angle region), the calculations performed give a criterion for selecting the modulation method to be applied. For the application to ac motor drives, for example, modulation method [4] would be more advantageous than method [5]. This is because, according to (32) and (34), in the whole modulation region for a phase-angle region from 40° to 140° (or -40° to -140°) the harmonic losses of method [4] are below the harmonic losses of [5].

IV. OPTIMAL MODULATION OF THE PWM CONVERTER FREQUENCY

The optimization of the continuous modulation can be reduced (as described in Section I) to a minimization of the local harmonic current rms value (cf. (15))

$$\begin{aligned} \Delta i_{N,RST,rms}^2 &= \Delta i_{N,RST,rms,1}^2 + \Delta i_{N,RST,rms,2}^2 \quad (59) \\ \frac{1}{\Delta i_n^2} \Delta i_{N,RST,rms,1}^2 &= \frac{48}{9} \delta_7 \{ \delta_2 \delta_6 (\delta_2 - \delta_6) - 2 \delta_{26} \\ &\quad \cdot [1 - (\delta_7 + \delta_6 + \delta_2)] \} \end{aligned}$$

$$\begin{aligned} \frac{1}{\Delta i_n^2} \Delta i_{N,RST,rms,2}^2 &= \frac{16}{9} \{ 6 \delta_{26}^2 + 2 \delta_{26} - 4 \delta_2^4 - 4 \delta_6^4 \\ &\quad - 4 \delta_2 \delta_{26} - 4 \delta_6 \delta_{26} - 8 \delta_2 \delta_6 \delta_{26} \\ &\quad + 2 \delta_2 \delta_6^2 - \delta_2^2 \delta_6 + 3 \delta_2^3 \delta_6 - \delta_2^2 \delta_6^2 \} \quad (60) \end{aligned}$$

with

$$\delta_{26} = \delta_2^2 + \delta_2 \delta_6 + \delta_6^2 \quad (61)$$

and

$$\delta_6 = \frac{\sqrt{3} M}{2} \sin \left(\varphi_U + \frac{\pi}{3} \right)$$

$$\delta_2 = \frac{\sqrt{3} M}{2} \sin \left(\varphi_U - \frac{\pi}{3} \right). \quad (62)$$

For the sake of simplicity in the following we only want to refer to the suboptimal solution (cf. (22) or method [2] in Fig. 5, respectively)

$$\delta_{7,[2]} = \frac{1}{2} [1 - (\delta_2 + \delta_6)]. \quad (63)$$

The dependency of the optimized local harmonic current rms value on the modulation depth M and phase φ_U of the converter voltage space vector is shown in Fig. 12. The characteristic shape of the global harmonic losses is given in Fig. 6 (cf. modulation method [2]). Fig. 12 shows a pronounced maximum in the upper modulation region in the vicinity of $\varphi_U = \pi/2$. Therefore, one has to raise the question whether or how for a given modulation depth M the shape of the harmonic power losses can be smoothed and thereby possibly the global harmonic power losses further reduced. The only remaining degree of freedom of the modulation method there is given by the variation of the pulse frequency that has been assumed constant (independently of φ_U) so far. Accordingly, the pulse frequency is to be increased in the region $\varphi_U \approx \pi/2$ and can be decreased in the regions $\varphi_U \approx \pi/3$ and $2\pi/3$.

The optimization of the pulse frequency shape $f_{P,FM}(\varphi_U)$ is expressed by a quality functional that has to be minimized:

$$\begin{aligned} I &= \\ &= \frac{1}{\Delta i_n^2} \int_{\frac{\pi}{3}}^{\frac{2\pi}{3}} \frac{1}{k_{f,FM}^2(\varphi_U, M, \varphi)} \Delta i_{N,RST,rms}^2(\varphi_U, M) d_U \\ &\quad \cdot I \rightarrow \text{Min}. \quad (64) \end{aligned}$$

The associated side condition is given by keeping the switching losses constant as they result for constant pulse frequency f_P according to

$$\begin{aligned} \frac{1}{2\pi} \int_{-\frac{\pi}{2}}^{+\frac{\pi}{2}} k_1 k_{f,FM}(\varphi_U, M, \varphi) f_P i_{N,R}(\varphi_U, \varphi) d_U &= \\ f_P \frac{k_1 \hat{I}_N}{\pi}. \quad (65) \end{aligned}$$

This means equal thermal stress on the power semiconductor devices. According to (65), the phase shift between converter output current and converter voltage again influences the determination of the switching losses, as already discussed in Section III. (The discontinuous modulation discussed there basically represents a special case of the general frequency modulation treated here.) Therefore, the optimization has to be performed for each phase angle φ and for each modulation depth M . The side condition (65) can be also written as

$$\int_{\frac{\pi}{3}}^{\frac{2\pi}{3}} k_{f,FM}(\varphi_U, M, \varphi) \zeta(\varphi_U, \varphi) d_U = 2 \quad (66)$$

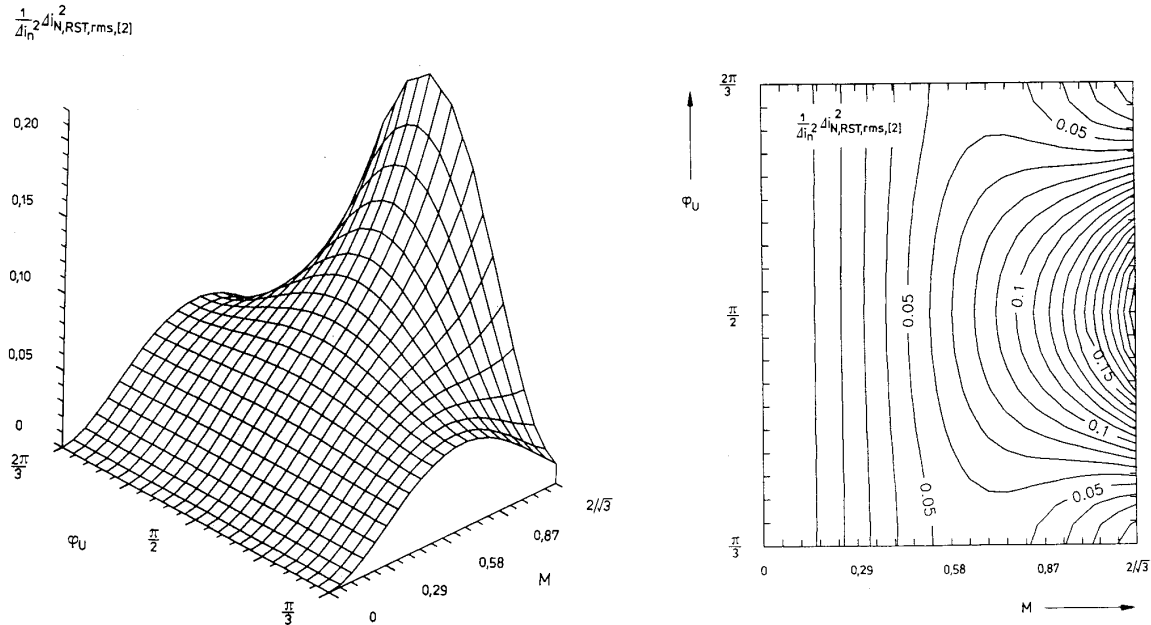


Fig. 12. Dependency of the normalized local harmonic power losses $\Delta i_{N,RST,rms}^2$ of the PWM converter system on the position φ_U of the converter voltage space vector and on the modulation depth M for suboptimal modulation [2] ((22), (61), and (62) have to be applied to (59)).

with

$$\zeta(\varphi_U, \varphi) = \left| \cos(\varphi_U + \varphi) \right| + \left| \cos\left(\varphi_U + \varphi - \frac{\pi}{3}\right) \right| + \left| \cos\left(\varphi_U + \varphi + \frac{\pi}{3}\right) \right|. \quad (67)$$

The weighting function ζ characterizing the influence of the sinusoidal current phase shift is shown in Fig. 13.

In general, the optimization problem treated here represents a problem of variational calculus: one has to calculate the shape of the relative (local) pulse frequency (the extremal)

$$k_{f,FM} = \frac{1}{f_p} f_{P,FM} = k_{f,FM}(\varphi_U, M, \varphi) \quad (68)$$

(for given M and φ) that minimizes the global harmonic power losses $\Delta I_{N,rms}^2(M, \varphi)$ where the side condition of constant switching losses is fulfilled. As a necessary condition for obtaining the extremal, one can give

$$\frac{\partial}{\partial k_{f,FM}} \left(\frac{1}{k_{f,FM}^2(\varphi_U, M, \varphi)} \frac{1}{\Delta i_n^2} \Delta i_{N,RST,rms}^2(\varphi_U, M) + \lambda k_{f,FM}(\varphi_U, M, \varphi) \zeta(\varphi_U, \varphi) \right) = 0 \quad (69)$$

according to the Euler-Lagrange differential equation of variational calculus. The side condition given as integral is linked to the calculation by the Lagrange multiplier λ . (As we know, this parameter is finally determined by inserting of the

extremal into the side condition (cf. [12]).) For the optimal frequency modulation there follows

$$k_{f,FM}(\varphi_U, M, \varphi) = \frac{2 \sqrt[3]{\frac{1}{\zeta(\varphi_U, \varphi)} \Delta i_{N,RST,rms}^2(\varphi_U, M)}}{\int_{\frac{\pi}{3}}^{\frac{2\pi}{3}} \sqrt[3]{\zeta^2(\varphi_U, \varphi) \Delta i_{N,RST,rms}^2(\varphi_U, M)} d\varphi_U} \quad (70)$$

(cf. Figs. 14 and 15). The necessary frequency sweep of the modulation is increased with increasing modulation depth and shows essentially a shape as already expected in the previous discussion. For a practical realization this frequency shape (in first approximation independent of the phase shift φ) can be approximated, e.g., by a simple sinusoidal or triangular modulation that is only dependent on M . The global harmonic power losses resulting for optimal frequency modulation are given in Fig. 16. We point out especially the dependency on φ ; no essential improvement of modulation method [2] (constant pulse frequency) is obtained, however. (Modulation method [2] is treated here as representative case; the other methods should show an equivalent result.)

If one also considers (besides the resulting harmonic power losses) the resulting noise of, e.g., an electric motor supplied by the converter, then the frequency modulation shows significant advantages as compared to a modulation method with constant pulse frequency. This results from the fact that the harmonics (which are concentrated in the immediate vicinity

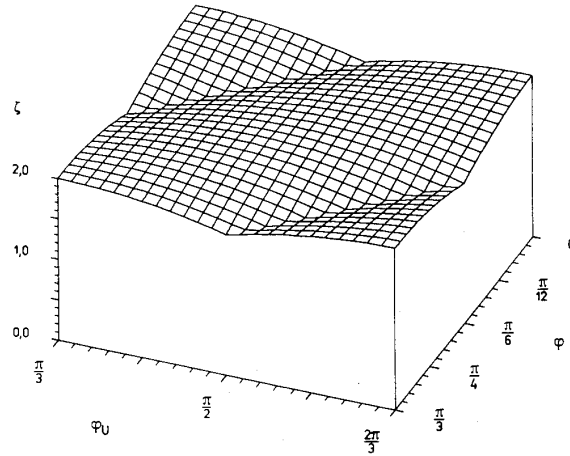


Fig. 13. Weighting factor ζ of the normalized local pulse frequency $k_{f,FM}$ for calculating the converter switching losses in dependency on the phase angle φ and on the angle φ_U (cf. (67)). Due to the symmetries of a purely sinusoidal balanced three-phase system the considerations can be limited to the interval $\varphi \in (0, \pi/3)$.

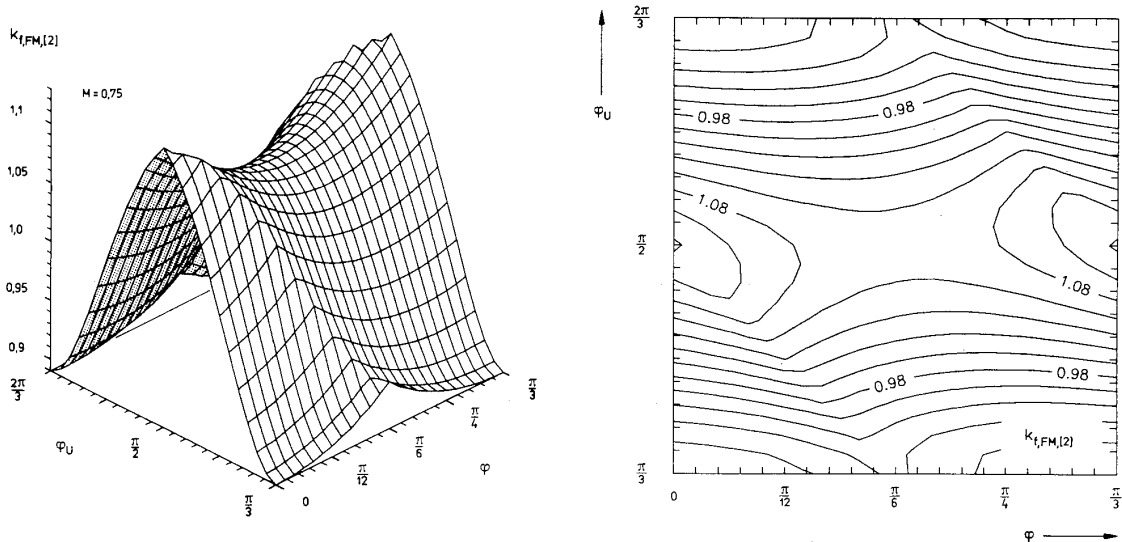


Fig. 14. Dependence of the optimal normalized frequency $k_{f,FM,[2]}$ of the pulse frequency modulation on the position $\varphi_U \in (\pi/3, 2\pi/3)$ of the converter voltage space vector and on the phase shift φ (referred to φ_U) of the converter output current; $M = 0.75$ (cf. (70)).

of multiples of the switching frequency for constant pulse frequency) are now distributed in frequency bands of the width

$$B \approx 2f_p(k_{f,FM} - 1). \tag{71}$$

Due to the equal spectral power (as we know, the spectral power is not influenced by frequency modulation), their amplitudes are decreased accordingly. There, the envelope of these spectral components for a large frequency sweep is defined by the shape of the modulating signal. There follows, e.g., for triangular modulation, an almost constant amplitude for the spectral components in the frequency regions defined by (71).

The resulting noise of the ac motor supplied by a PWM converter, therefore, is distributed in a wider frequency band as compared to modulation methods with constant pulse frequency. There do not appear to be pronounced audible frequencies with multiples of the pulse frequency.

V. CONCLUSIONS

The main topic of this paper is the determination of those power loss components of a PWM converter system that can be (besides the harmonic losses) influenced by the modulation method selected. Those power loss components are usually neglected in pulse pattern optimization methods known from

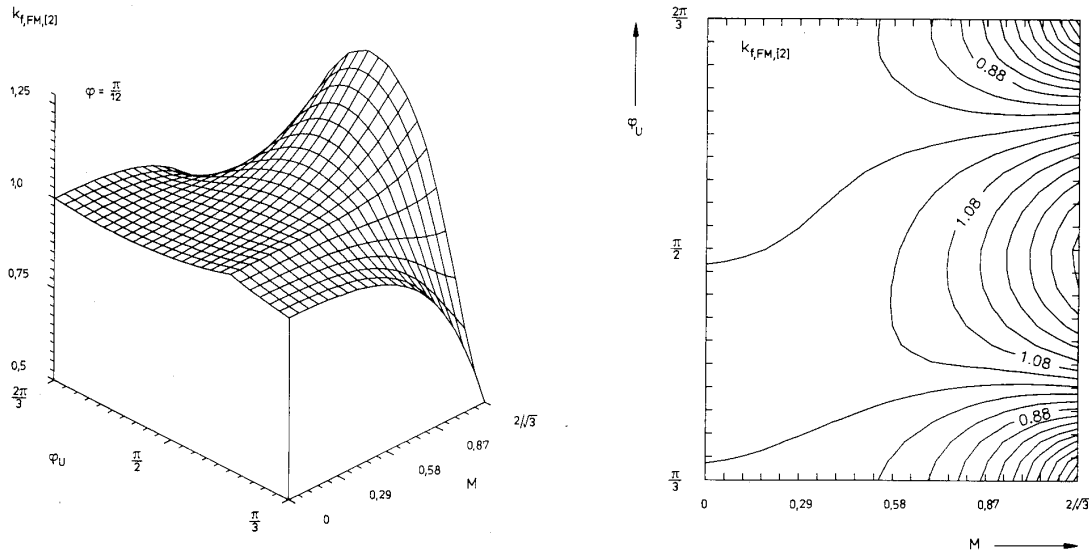


Fig. 15. Dependency of the optimal normalized frequency $k_{f,FM,[2]}$ of the pulse frequency modulation on the position $\varphi_U \in (\pi/3, 2\pi/3)$ of the converter voltage space vector and on the modulation depth M ; $\varphi = 0$ (cf. (70)).

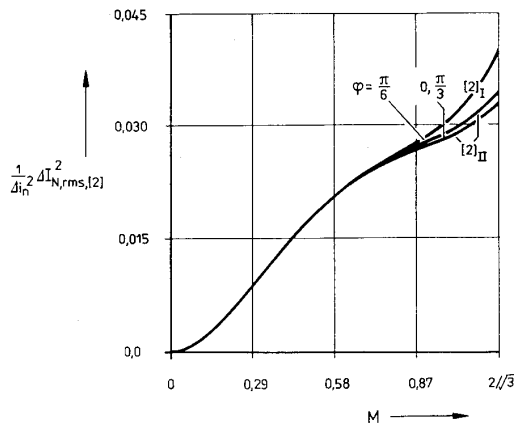


Fig. 16. Comparison of the normalized global harmonic losses of one phase for constant (denoted by $[2]_I$) and modulated (denoted by $[2]_{II}$) converter pulse frequency. The comparison is made for equal global switching losses in both cases to given a common basis for the comparison. (Parameter of the family of curves: phase angle φ of the output current.)

the literature because the optimization is performed with the side condition of a given average (global) switching frequency, but not with the essential side condition of defined global switching losses.

If the assumption of sufficient thermal inertia of the power semiconductor devices is not fulfilled any further (meaning low output frequencies), one has to include a dynamic thermal model (transient thermal resistance) for the power electronic devices into the optimization procedure for considering the device behavior with respect to the switching and conduction losses within the fundamental period. A pulse pattern optimization would then be thinkable, e.g., with the side condition of a maximum allowable chip temperature.

For the optimization of the stationary behavior of an ac motor drive system (the final goal of a pulse pattern optimization) one should generally check to see whether a detailed modeling limited only to the motor is sufficient. One has to consider also the loss contributions mentioned in this paper and therefore especially the converter losses. It would be not advisable to optimize a few percent of harmonic motor power losses (which are small for high pulse frequencies in any case) if one would not also consider the possibly (much) higher influences on the losses of the converter due to the nonideality of the power electronic devices.

ACKNOWLEDGMENT

The authors are very much indebted to the Austrian Fonds zur Förderung der Wissenschaftlichen Forschung, which supports the work of the Power Electronics Section at the Technical University Vienna.

REFERENCES

- [1] S. Halász, "Voltage spectrum of pulse-width-modulated inverters," Technical University Budapest, *Periodica Polytechnica, Elect. Eng.*, vol. 25, no. 1, pp. 135-145, 1981.
- [2] J. W. Kolar, H. Ertl, and F. C. Zach, "Analytically closed optimization of the control method of a PWM rectifier system with high pulse rate," in *Proc. PCIM'90* (Munich, Germany), June 27-29, 1990, pp. 209-223.
- [3] S. R. Bowes and A. Midoun, "Suboptimal switching strategies for microprocessor-controlled PWM inverter drives," in *Proc. Inst. Elec. Eng.*, vol. 132, pt. B, no. 3, pp. 133-148, 1985.
- [4] G. Buja and G. Indri, "Improvement of pulse width modulation techniques," *Archiv für Elektrotechnik*, vol. 57, pp. 281-289, 1977.
- [5] H. W. van der Broeck, H. C. Skudelny, and G. V. Stanke, "Analysis and realization of a pulsewidth modulator based on voltage space vectors," *IEEE Trans. Industry Appl.*, vol. IA-24, no. 1, pp. 142-150, 1988.
- [6] Y. Ikeda, J. Itsumi, and H. Funato, "The power loss of the PWM voltage-fed inverter," in *19th PESC '88 Conf. Rec.* (Kyoto, Japan), vol. 1, Apr. 11-14, 1988, pp. 277-283.

- [7] J. Nishizawa, T. Tamamushi, and K. Nonaka, "The experimental and theoretical study on the high frequency and high efficiency SI thyristor type sinusoidal PWM inverter," in *Proc. 14th PCI'87 Conf.* (Long Beach, CA), Sept. 14-17, 1987, pp. 167-181.
- [8] J. W. Kolar, H. Ertl, and F. C. Zach, "Calculation of the passive and active component stress of three-phase PWM converter systems with high pulse rate," in *Proc. 3rd European Conf. Power Electron. Appl.* (Aachen, Germany), Oct. 9-12, 1989, vol. 3, pp. 1303-1311.
- [9] L. K. Mestha and P. D. Evans, "Optimization of losses in PWM inverters," *IEE Conf. Publ.*, no. 291, 1988, 394-397.
- [10] J. H. Rockot, "Losses in high-power bipolar transistors," *IEEE Trans. Power Electron.*, vol. PE-2, no. 1, pp. 72-80, 1987.
- [11] B. Sneyers, Ph. Lataire, G. Maggetto, B. Detemmerman, and J. M. Bodson, "Improved voltage source GTO inverter with new snubber design," in *2nd European Conf. Power Electron. Appl.* (Grenoble, France), Sept. 22-24, 1987, vol. 1, pp. 31-36.
- [12] F. Zach, *Technisches Optimieren*. Vienna-New York: Springer-Verlag, 1974.



Johann W. Kolar was born in Upper Austria on July 15, 1959. He is currently working on the Ph.D. degree in the area of control optimization of single-phase and three-phase PWM rectifier systems and switched-mode power supplies.

He is with the Power Electronics Section of the Technical University Vienna. He also does research in the areas of inverter and converter development and the theoretical analysis of power electronic systems. He is the author of numerous technical and scientific papers and patents.



Hans Ertl was born in Upper Austria on May 28, 1957. He received the Dipl.Ing. (M.Sc.) degree from the Technical University Vienna, Austria, in 1984. As a Scientific Assistant of the Power Electronics Section, he presently is finishing his Ph.D. thesis in the area of three-phase PWM converter systems.

He also does research concerning the analysis and design of switched mode power supplies. He is the author of various technical and scientific papers and patents.



Franz C. Zach (M'82) was born in Vienna, Austria, on December 5, 1942. He received the Dipl.-Ing. (M.Sc.) and Ph.D. degrees (cum laude) from the University of Technology, Vienna, Austria, in 1965 and 1968, respectively.

From 1965 to 1969 he was a Scientific Assistant in Vienna, and from 1969 to 1972 he was with the NASA Goddard Space Flight Center in Greenbelt, MD (Washington, DC). In 1972 he returned to Austria to become Associate Professor for Power Electronics at the Vienna University of Technology. There he has been heading the Power Electronics Section since 1974. He is the author of numerous technical and scientific papers and patents and of two books on automatic control and on power electronics. His current activities lie in power electronics and associated controls, especially as used for variable-speed ac and dc motor drives and for power supplies. He is also involved in extensive industrial work in these areas.